Front. Earth Sci. 2013, 7(4): 487–500
DOI 10.1007/s11707-013-0392-9

RESEARCH ARTICLE

Carbonate formation and water level changes in a paleo-lake and its implication for carbon cycle and climate change, arid China

Yu LI (✉), Nai'ang WANG, Zhuolun LI, Xuehua ZHOU, Chengqi ZHANG, Yue WANG

College of Earth and Environmental Sciences, Center for Hydrologic Cycle and Water Resources in Arid Region, Lanzhou University, Lanzhou 730000, China

Abstract Carbonate deposition is a main inorganic carbon sink in lakes, which varies depending on climate change and internal lake dynamics. Research on the relationship between lake carbonate and climate will help to understand mechanisms of carbon cycle in lacustrine systems. The approach of this study is to explicitly link carbonate formation with Holocene long-term climate change and lake evolution in a paleo-lake (Zhuye Lake), which is a terminal lake of a typical inland drainage basin in arid China. This paper presents analysis on grain-size, carbonate content and mineralogical composition of sediment samples from different locations of Zhuye Lake. The results show that calcite and aragonite are two main components for the lake carbonate, and the carbonate enrichment is associated with lake expansion during the Late Glacial and early to middle Holocene. Holocene lake expansion in arid regions of China is usually connected with high basin-wide precipitation that can strengthen the basin-wide surface carbonate accumulation in the terminal lake. For this reason, Zhuye Lake plays a role of carbon sinks during the wet periods of the Holocene.

Keywords carbonate, carbon cycle, lake sediments, mineralogical composition, climate change

1 Introduction

Lakes are dynamic response systems that integrate environmental, climatic, and tectonic forcings into a continuous, high-resolution archive of local and regional change (Gierlowski-Kordesch and Kelts, 1994). Affected by basin-wide climate factors, such as precipitation, aridity, windiness, and mean summer temperature, as well as geographical and geological conditions, lakes exhibit enormous physico-chemical variability, which acts to influence the sedimentation and carbon cycle into the various lacustrine environments (Meyers and Ishiwatari, 1993; Lenton, 2000; Schnurrenberger et al., 2003). Carbonate is a main inorganic carbon sink in lake sediments, and its variability is controlled by different climate factors according to locations and climate zones (Gorham et al., 1983; McConnaughey et al., 1994; Dean, 1999). Carbonate content in lake sediments is also influenced by organic carbon concentration in the carbon cycle, because carbonate may dilute the concentration of organic matter somewhat and produce calcareous sediments (Meyers and Ishiwatari, 1993; Dean, 1999). Furthermore, sub-aquatic springs also can have a large potential to affect hydrological conditions, thereby affecting carbonate formation in lake sediments (Matter et al., 2010). Study on mechanisms of lake carbonate formation and its relationship with climate change is important to the understanding of the terrestrial carbon cycle system.

There are numerous lakes in arid and semiarid regions of China, while saline lakes account for more than half of those lakes (Hammer, 1986; Wang, 1987; Williams, 1991). Carbonate minerals are commonly found in the lakes of western and central China, and their content is closely correlated with climatic factors (Zheng et al., 1993; China Meteorological Administration, 1994; Zheng et al., 2000). In addition, carbonate is also widely found in the Holocene lake sediments from East Asia and the Qinghai-Tibet Plateau: e.g., Hulun Lake (Wen et al., 2010), Bayanchagan Lake (Jiang and Liu, 2007), Dali Lake (Xiao et al., 2008), Daihai Lake (Xiao et al., 2004; Peng et al., 2005), Qinghai Lake (Shen et al., 2005; Liu et al., 2007), Chaka Lake (Liu et al., 2008a), Koucha Lake (Mischke et al., 2010), Ahung

Received January 30, 2013; accepted May 6, 2013

E-mail: liyu@lzu.edu.cn

Co (Morrill et al., 2006), Sumxi Co (Gasse et al., 1991), Seling Co (Morinaga et al., 1993). Proxies, such as grain-size (Peng et al., 2005), pollen (Xiao et al., 2004), oxygen isotope (Liu et al., 2007), and organic geochemistry (Morrill et al., 2006), have been successfully used for paleo-environment reconstruction in those Holocene lake sediments. However, little research has been devoted to the relationship between inorganic carbon cycle and climate change, which is an important field for long-term terrestrial carbon cycle study in arid and semiarid regions of China. Zhuye Lake, the terminal lake of the Shiyang River drainage basin, is located in the marginal region of the Asian summer monsoon, where the climate is sensitive to the advancing and retreating of the monsoon (Fig. 1). Zhuye Lake is a typical paleo-lake in arid China, and long-term carbon cycle and climate change research in the drainage basin is useful in understanding the terrestrial carbon cycle in inland drainage basins, which are widely distributed in arid China. Much work has been carried out on late Quaternary lake evolution and climate change (Pachur et al., 1995; Chen et al., 2003, 2006; Zhang et al., 2004; Zhao et al., 2008; Li et al., 2009). Few researchers have studied the long-term basin-wide carbon cycle by carbonate research in lake sediments. The objective of the present paper is to obtain carbonate content variability in the lake basin and to study the links between climate change and carbonate formation. Carbonate content and mineralogical composition of lake sediments vary according to lake saline zones (Schmalz, 1966; Sun, 1990; Liu et al., 2006). It is therefore required to examine carbonate content in different locations of a lake basin for understanding carbon content variability in lake sediments. This paper presents carbonate content and mineralogical composition of sediment samples from five sections in the different locations of Zhuye Lake, arid China. Organic matter, pollen concentrates and mollusk shells were used for conventional and AMS ^{14}C radiocarbon dating in the five sections. Sediment lithology and grain-size were also used to infer lake evolution. Furthermore, the basin-wide geochemical and physical controls on carbonate production were also discussed in this study.

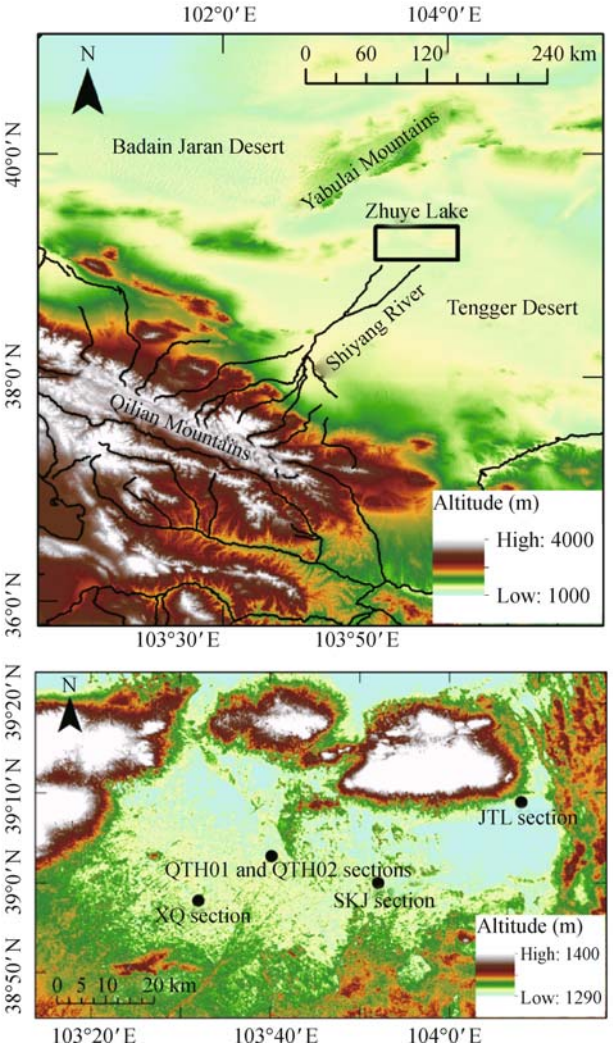

Fig. 1 Map showing latitudes, longitudes and elevations in the Shiyang River drainage area and Zhuye Lake. Black solid circles indicate the locations of the QTH01, QTH02, XQ, SKJ and JTL sections.

2 Regional setting

In the Eastern Qilian Mountains, the Shiyang River drainage area is roughly at geographical coordinates of 100°57'E–104°57'E, 37°02'N–39°17'N. The length of the drainage path is about 300 km and the total area is 4.16×10^4 km^2 (Fig. 1). Zhuye Lake, the terminal lake of the drainage area, is a tectonic rift basin, belonging to the Qilian Mountains piedmont fault basin (Fig. 1). The Quaternary unconsolidated lacustrine and alluvial can reach up to 300 m thick in the basin (Chen and Qu, 1992). The Shiyang River drainage area is located in the transition zone of monsoonal and arid regions according to the geographical divisions of China, while the modern climate in this area is affected by the combined effect of the Asian monsoon and the westerly winds (Zhao, 1983; Wang et al., 2005a). The Shiyang River drainage area can be divided into three climatic zones from south to north. (i) The alpine semi-arid area of the Qilian Mountains has an altitude of 2000–5000 m, annual rainfall of 300–600 mm, and annual evaporation of 700–1200 mm. (ii) The cool and arid central plains have an altitude of 1500–2000 m, annual rainfall of 150–300 mm, and annual evaporation of 1300–2000 mm. (iii) The northern warm and dry area has an altitude of 1300–1500 m, annual rainfall less than 150 mm, and annual evaporation of 2000–2600 mm (Chen and Qu, 1992). HCO^{3-} and Ca^{2+} are dominant ions in basin-wide precipitation. In the upper reaches of the drainage area, the chemical composition of groundwater is consistent with that of precipitation, and the salinity is less than 0.3 g/L.

The contents of these ions, such as Cl^-, SO_4^{2-}, Na^+, Ca^{2+}, and Mg^{2+}, increase with the decreased altitude & precipitation and increased evaporation in the drainage area, while the groundwater salinity increases accordingly (Ding and Zhang, 2005). Therefore, the groundwater chemical composition is mainly controlled by elevation, which leads to change in the precipitation-evaporation ratio. The chemical composition of the basin-wide surface water also shows a similar trend compared with that of the groundwater (Ding and Zhang, 2005). Zhuye Lake has been dry since the 1950s due to climate change and human impact. At present, only the northeast part of the lake still has a small amount of water during the summer season.

3 Materials and methods

Sediment samples from five sections in the Zhuye Lake basin, the Xiqu section (XQ, 38°58'N 103°32'E, Altitude: 1316 m, Depth: 8.50 m), the Qingtuhu01 section (QTH01, 39°03'N 103°40'E, Altitude: 1309 m, Depth: 6.92 m), the Qingtuhu02 section (QTH02, 39°03'N 103°40'E, Altitude: 1309 m, Depth: 6.92 m), the Shakenjing section (SKJ, 39°00'N 103°52'E, Altitude: 1305 m, Depth: 3.55 m), the Jiutuoliang section (JTL, 39° 09'N 104° 08'E, Altitude: 1308 m, Depth: 3.00 m), were collected for a study of grain-size, carbonate content, and mineralogical composition. The QTH02 and JTL sections were sampled at 2 cm and 10 cm intervals, and the XQ and SKJ sections were sampled at 5 cm intervals. The QTH01 section was sampled at 2 cm intervals in lacustrine layers and 5 cm intervals in other layers. Figure 1 shows the topography of the lake and locations of the five sections, and Figure 2 indicates the lithology of the five sections.

Organic matter, pollen concentrates and mollusk shells were selected for conventional and AMS ^{14}C radiocarbon dating to establish lake sediment chronologies in the QTH01, QTH02, XQ, SKJ, and JTL sections (Table 1). The conventional ^{14}C dates were measured at the radiocarbon dating laboratory of Lanzhou University, and the AMS ^{14}C dates were measured at the Dating Laboratory of Peking University. Pollen concentrates as materials for AMS ^{14}C dating were extracted by treatment with acid and alkali, then sieving for enriching (Brown et al., 1989; Moore et al., 1991; Zhou et al., 1999). Dating samples of the pollen concentrates were checked under a microscope, then samples with plenty of aquatic plant pollen and celluloses were excluded.

Grain-size distribution of all samples was determined by the Malvern Mastersizer 2000 particle analyzer that automatically yields the percentages of clay-, silt- and sand-size fractions, as well as median, mean and mode sample diameters. Sediments (0.2–0.4 g) were pretreated by heating in 10 mL of 10% H_2O_2 to remove organics, heated in 10 mL 10% HCl to remove carbonate that otherwise would bond different mineral fractions, then shaken in Na-hexametaphosphate to disaggregate the sediment for 1 hr prior to analysis.

X-ray diffraction (XRD) is a rapid analytical technique primarily used for phase identification of a crystalline material and can provide information on mineral composition of sediment samples. The PANalytical X'Pert Pro MPD (Multi Purpose Diffractometer) was used for analysis of carbonate content and mineral composition. The instrument is equipped with a Cu X-ray tube source and a vertical circle theta:theta goniometer with a radius of 240 mm. This configuration keeps the stationary sample horizontal during data collection. The X'Pert PRO systems with the X'Celerator detector allow the rapid collection of hundreds of scans in a very short time. Test procedures require sieved sediment; therefore, sediment samples (2.0 g) were sieved through a 37 micron sieve then powdered. A set of 158 sediment samples (65, 26, 29, 21, and 17 samples from the QTH01, QTH02, XQ, SKJ, and JTL sections, respectively) were pretreated for the analysis. For mineral identification, we used X'Pert HighScore Plus software and calculated the percentage values of each mineral by the respective RIR values. In this study, the carbonate content is calculated by the sum of all carbonate minerals (aragonite, calcite, and dolomite), while the feldspar content is the sum of all feldspar minerals.

4 Results

4.1 Lithology and grain-size

Lacustrine sediments in Zhuye Lake are characterized mainly by gray silt mixed with brown and black layers. Gray or brown sand layers are always embedded in lacustrine sediments, indicating changes of the lake level and hydrodynamic conditions. The top of each section is usually covered with Late Holocene eolian sediments of uneven thickness. According to the lithology, these eolian sediments, which have a loose structure and without characteristics of oxidation or reduction that can usually be seen underwater, are similar to modern top eolian deposits in surroundings, illustrating the retreating lake. Some layers of the lacustrine sediments are rich in carbonate, snails, and shells according to our field investigations. Figure 2 shows the lithology of the QTH01, QTH02, XQ, SKJ, and JTL sections. The results of grain-size analysis show that silt (%, 4–63 μm) is the major component of the lacustrine layers, and the median grain-size can reflect the general variability of the lithology and grain-sizes; therefore, these two grain-size parameters are chosen to imply the lithology and lake sediment particle size changes (Figs. 3–7 and Table 2). In addition, the purpose of using grain-size data in this study is to evaluate the overall sediment

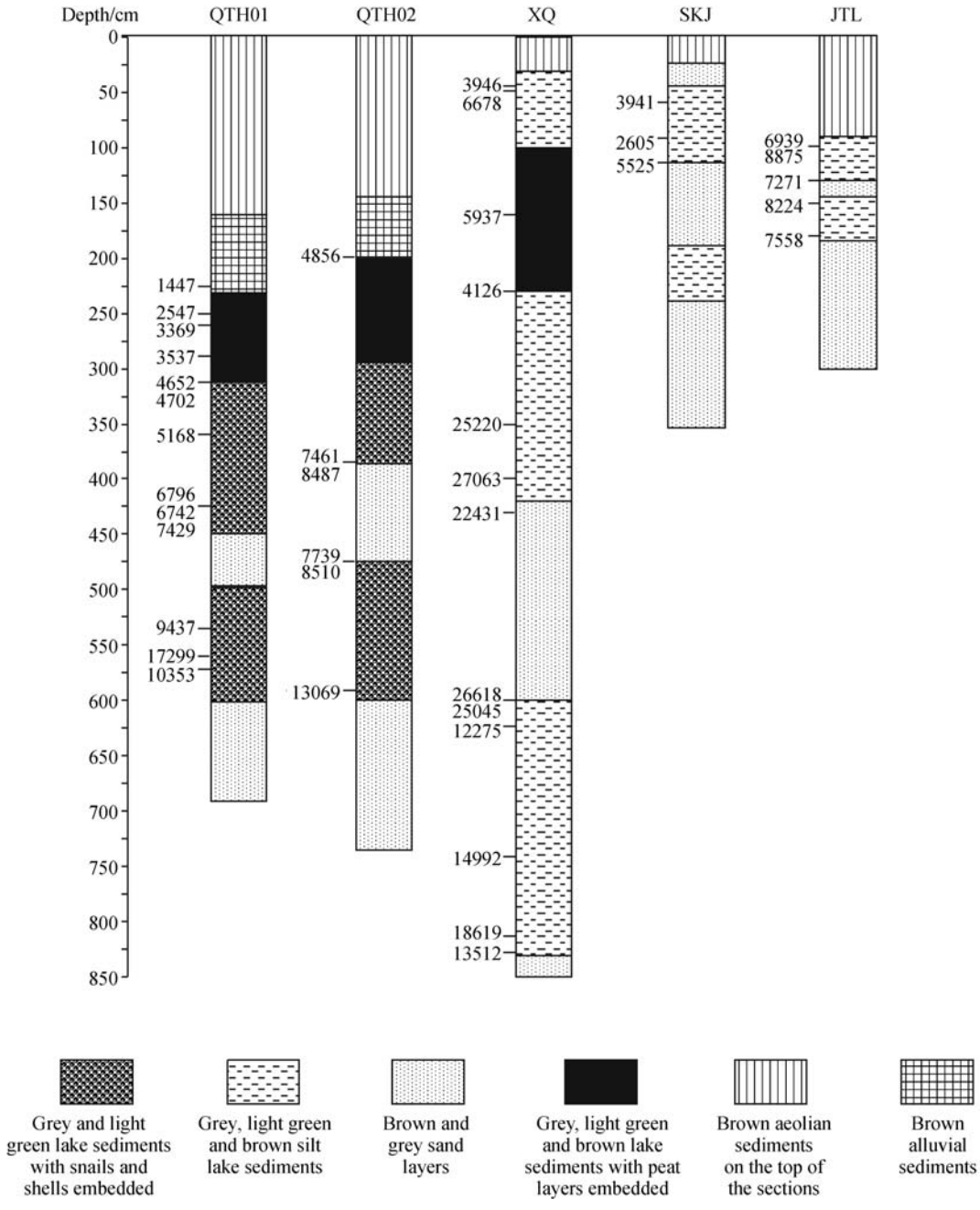

Fig. 2 Lithology and the calibrated ^{14}C dates (cal yr BP) for the QTH01, QTH02, XQ, SKJ and JTL sections.

particle size, which reflects the water level changes. After comparing all the grain-size parameters (including clay contents, sorting coefficients, kurtosis, and skewness), the median values and silt contents can indicate the overall sediment particle conditions very well. As shown in these figures, the median grain-size is relatively low and the silt content is relatively high in the typical lacustrine layers of the five sections. On the different time scales, grain-size of lake sediments indicates variable climatic information. On the interannual-scale, coarse lake sediments can be related to basin-wide high precipitation and runoff. However, on the centennial-to-millennial scale, it is described as the sediment sorting principle that the grain-size of lake sediments becomes finer and finer from the shore to the center, and sediment belts of different grain-size fractions levels can be distinguished; as a result, the grain-size of lake sediments is in close relation to water level and the energy of the inflows (Lerman, 1978; Chen et al., 2004). Grain-size variations in this study, therefore, reflect millennial-scale long-term changes in the processes and energy of sediment transport, which are closely related to lake levels. According to the lithology of the five sections,

Table 1 Conventional and AMS ^{14}C dates for the QTH01, QTH02, XQ, JTL and SKJ sections.

Section	Laboratory number	Depth/m	Dating materials	^{14}C age/yr BP	Calibrated ^{14}C age (2σ)/cal yr BP
QTH01	LUG96–44	2.25	Organic matter	1550 ± 60	1316–1551(1447)
	LUG96–45	2.50	Organic matter	2470 ± 90	2351–2740(2547)
	BA05223	2.62	Shells	3140 ± 40 (AMS)	3263–3448(3369)
	LUG96–46	2.90	Organic matter	3300 ± 90	3356–3821(3537)
	LUG96–47	3.15	Organic matter	4130 ± 110	4298–4953(4652)
	BA05224	3.15	Shells	4160 ± 40 (AMS)	4571–4831(4702)
	LUG96–48	3.60	Organic matter	4530 ± 80	4881–5449(5168)
	LUG96–49	4.25	Inorganic matter	5960 ± 65	6652–6953(6796)
	BA05225	4.25	Shells	5920 ± 40 (AMS)	6658–6854(6742)
	BA101234	4.25	Pollen concentrates	6510 ± 40(AMS)	7322–7494(7429)
	LUG02–25	5.37	Organic matter	8412 ± 62	9293–9530(9437)
	BA101237	5.61	Pollen concentrates	14220 ± 50(AMS)	16989–17599(17299)
	LUG02–23	5.72	Organic matter	9183 ± 60	10234–10502(10353)
QTH02	BA101254	1.99	Pollen concentrates	4300 ± 25(AMS)	4830–4958(4856)
	BA05222	3.88	Shells	6550 ± 40 (AMS)	7344–7563(7461)
	BA101256	3.88	Pollen concentrates	7705 ± 35(AMS)	8413–8575(8487)
	BA05221	4.75	Shells	6910 ± 40 (AMS)	7671–7833(7739)
	BA101257	4.75	Pollen concentrates	7735 ± 35(AMS)	8432–8587(8510)
	BA05218	5.91	Shells	11175 ± 50 (AMS)	12875–13241(13069)
XQ	Zhao (2005)	0.45	Organic matter	3628 ± 58	3731–4144(3946)
	BA101249	0.48	Pollen concentrates	5855 ± 30(AMS)	6567–6745(6678)
	Zhao (2005)	1.62	Organic matter	5176 ± 68	5746–6177(5937)
	Zhao (2005)	2.28	Organic matter	3758 ± 65	3926–4405(4126)
	Zhao (2005)	3.51	Organic matter	21101 ± 220	24539–25862(25220)
	BA101248	3.98	Pollen concentrates	22380 ± 100(AMS)	26301–27716(27063)
	Zhao (2005)	4.29	Organic matter	18803 ± 207	21816–23290(22431)
	Zhao (2005)	6.00	Organic matter	22158 ± 189	26052–27580(26618)
	BA101247	6.03	Pollen concentrates	21000 ± 120(AMS)	24575–25510(25045)
	Zhao (2005)	6.23	Organic matter	10400 ± 80	12029–12555(12275)
	Zhao (2005)	7.42	Organic matter	12688 ± 117	14237–15572(14992)
	BA101246	8.13	Pollen concentrates	15360 ± 60(AMS)	18499–18792(18619)
	Zhao (2005)	8.27	Organic matter	11650 ± 110	13290–13753(13512)
JTL	LUG–03–08	0.98	Organic matter	6071 ± 80	6744–7162(6939)
	BA101253	1.00	Pollen concentrates	8000 ± 40(AMS)	8663–9009(8875)
	LUG–03–07	1.29	Organic matter	6350 ± 114	6987–7475(7271)
	LUG–03–06	1.50	Organic matter	7410 ± 140	7952–8454(8224)
	LUG–03–05	1.81	Organic matter	6688 ± 100	7419–7732(7558)
SKJ	BA101239	0.58	Pollen concentrates	3630 ± 25(AMS)	3866–4070(3941)
	Zhao (2005)	0.93	Organic matter	2541 ± 57	2366–2759(2605)
	Zhao (2005)	1.14	Organic matter	4808 ± 70	5324–5659(5525)

the layers with many coarse components indicate shallow lacustrine deposits. As a result, the overall trend of the median grain-size reflects the millennial-scale lake level changes. Research on the modern lake sediments grain-size shows that silt is a main component for suspended load in lakes and rivers (Sun et al., 2002). Therefore, silt content can be seen as a proxy showing the hydrodynamic conditions of Zhuye Lake. High silt contents are commonly accompanied by relatively low median grain-size in the five sections, which shows that the high suspended load is associated with lake expansion. Generally, the average median grain-size and silt content are 68.28 μm and 46.35% for the QTH01 section, 79.40 μm and 38.21% for the QTH02 section, 50.43 μm and 43.05% for the XQ section, 125.50 μm and 18.43% for the SKJ section, and 137.21 μm and 25.08% for the JTL section. Sediments in the QTH01, QTH02, and XQ sections are relatively finer than those from the SKJ and JTL sections. Lake hydrodynamic conditions are different in different parts of a lake basin, which can result in the uneven sediment grain-size distribution. The QTH01, QTH02, SKJ, and JTL sections can be divided into five phases (A, B, C, D, and E) on the basis of lithology, silt content, and median grain-size (Figs. 3–7 and Table 2). Among these 5 phases, phase E is usually characterized by top eolian sediments; typical lacustrine sediments are abundant in the B and D phases, while sand content is relatively high in the A and C phases revealing shallow lacustrine sediments. There are four phases in the XQ section; the phases A and C are typical lacustrine sediments; the phases B and D are

Table 2 Percentages of silt content (%), median grain-size (μm), carbonate content (%) and main mineralogical component for different phases in the QTH01, QTH02, XQ, SKJ and JTL sections.

	Calcite/%	Aragonite/%	Carbonate/%	Feldspar/%	Median/μm	Silt/%	Quartz/%	Albite/%	Muscovite/%	Anorthite/%
QTH01	16.65	6.32	23.85	24.42	68.28	46.35	21.40	13.55	15.57	7.37
A(QTH01)	1.00	0.00	1.00	36.17	155.99	14.29	42.17	10.67	3.67	21.00
B(QTH01)	9.44	13.22	23.56	30.44	77.63	40.91	17.89	19.78	16.78	5.44
C(QTH01)	7.60	3.80	11.40	38.20	128.28	8.07	19.20	25.80	23.80	7.00
D(QTH01)	38.39	11.87	50.35	11.87	36.61	59.69	11.09	6.83	4.83	4.39
E(QTH01)	3.18	0.00	5.32	28.73	35.92	62.55	28.45	16.05	27.68	7.64
QTH02	17.58	10.12	28.12	20.92	79.40	38.21	20.73	16.69	6.73	3.04
A(QTH02)	10.00	5.00	15.50	21.25	187.41	5.30	24.00	18.00	7.50	3.25
B(QTH02)	14.60	15.20	31.00	15.00	49.83	47.92	18.80	15.00	11.40	0.00
C(QTH02)	15.00	10.00	25.33	37.67	129.51	8.64	22.33	28.67	9.67	0.00
D(QTH02)	33.88	17.13	51.00	10.38	41.38	51.26	14.75	9.13	4.13	1.25
E(QTH02)	4.67	0.00	5.00	31.33	36.52	55.78	27.33	21.33	4.33	9.33
XQ	3.19	0.00	3.33	28.14	50.43	43.05	28.14	15.24	26.67	7.33
A(XQ)	3.29	0.00	3.29	31.71	9.24	48.66	24.29	13.14	25.43	11.57
B(XQ)	1.00	0.00	1.20	37.40	156.01	6.75	34.60	16.80	16.80	14.60
C(XQ)	4.71	0.00	5.00	20.43	16.99	59.23	27.43	15.86	32.57	0.00
D(XQ)	3.00	0.00	3.00	19.50	143.04	15.93	28.00	16.50	35.00	0.00
SKJ	3.52	0.00	3.52	33.95	125.50	18.43	26.00	14.81	22.52	13.86
A(SKJ)	0.00	0.00	0.00	31.83	172.30	5.37	27.00	13.67	24.83	13.83
B(SKJ)	14.00	0.00	14.00	37.33	102.89	27.69	23.00	16.33	12.00	14.00
C(SKJ)	0.00	0.00	0.00	28.00	136.86	10.14	28.33	12.67	26.67	11.33
D(SKJ)	4.25	0.00	4.25	29.00	88.95	31.31	25.25	11.75	28.25	10.75
E(SKJ)	3.00	0.00	3.00	42.00	80.55	30.65	25.80	19.00	19.00	17.80
JTL	3.35	4.59	8.12	31.12	137.21	25.08	23.94	16.76	28.06	8.53
A(JTL)	2.40	0.00	2.40	31.20	210.83	7.55	32.20	17.40	25.00	6.40
B(JTL)	3.33	0.00	4.00	37.67	25.47	68.80	6.33	22.00	39.00	8.67
C(JTL)	1.50	1.50	3.00	32.50	159.83	13.77	28.50	14.00	28.50	8.50
D(JTL)	8.33	23.67	32.00	14.67	40.73	57.26	16.67	10.33	29.67	4.33
E(JTL)	1.75	1.00	3.00	37.75	138.88	15.14	30.00	18.25	22.25	14.25

shallow lacustrine deposits and aeolian sediments respectively. As has been shown in Table 2, grain-size phases and variability are clear according to the data of silt content and median grain-size. In the shallow lacustrine deposits, the silt content is usually less than 20%, and the median grain-size is generally larger than 100 μm, while the typical lacustrine deposits are abundant with fine components showing lake expansion and more suspended load.

4.2 Chronology

Table 1 and Fig. 2 show the conventional and AMS ^{14}C ages from the five sections, and Figs. 3–7 indicate dates and different phases in every section. Overall, sediments from the five sections are formed mostly during the Late Glacial and Holocene. The QTH01 and QTH02 sections are located in the central part of Zhuye Lake (Fig. 1). The ages of different dating materials are relatively consistent with each other. The typical lacustrine sediment phases B (~13.0–~7.7 cal kyr BP) and D (~7.4–~4.8 cal kyr BP) are formed during the early and middle Holocene in the two sections. The phase C, a sand layer, is formed ~7.5 cal kyr BP. In the SKJ section, which is also located in the middle of the lake (Fig. 1), the upper typical lacustrine layer (phase D) was formed between ~5.5–~4.0 cal kyr BP and the lower typical lacustrine layer (phase B) can be correlated with the early Holocene lacustrine layer in the QTH01 and QTH02 sections. The JTL section is located in the eastern part of Zhuye Lake (Fig. 1). Four bulk organic matter ages were generally consistent, but slightly inverted. The four bulk organic matter ages and one age from pollen concentrates show that the typical lacustrine sediments (phases B and D) are formed during the early-to-mid-Holocene, ~8.0 cal kyr BP. The XQ section is located in the west of Zhuye Lake and close to the estuary (Fig. 1), and the ages from this section are more complicated than other sections. The lower lacustrine layer (phase A) is formed during the Late Glacial according to the ages; however, five ages from the middle of the section (phases B and C) are much older than the ages from the lower part. At the western edge of the lake, the sediment reworking effect, which is related to strong runoff and lake waves, can affect the ages of the XQ section. Based on the ages from the bottom typical lacustrine sediments, the typical lacustrine sediments (phases A and C) correspond to the phases B and D in the QTH01 and QTH02 sections; therefore, most of the typical lacustrine sediments are also formed during

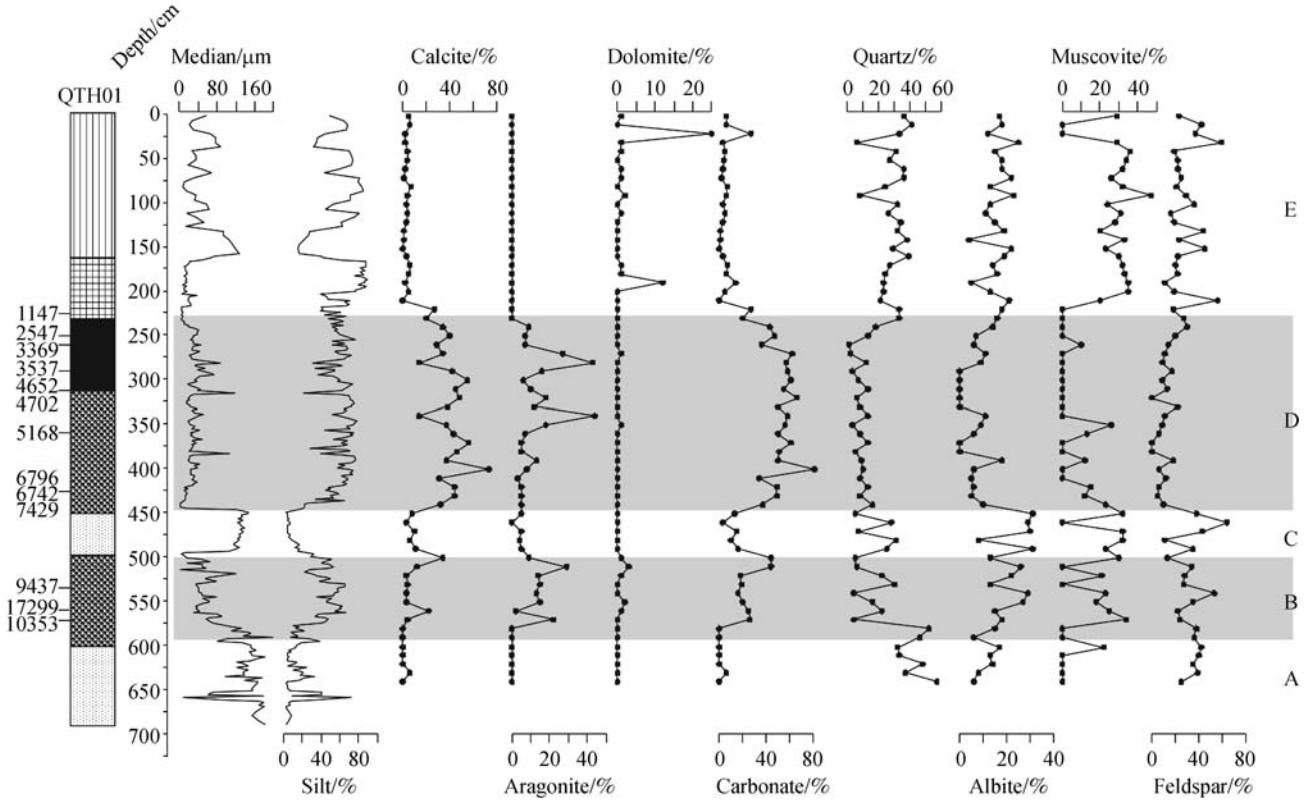

Fig. 3 Percentages of silt content (%), median grain-size (μm), carbonate content (%) and main mineralogical component in the QTH01 section, plotted against the depth. The grey bars indicate typical lacustrine layers with high carbonate content. The section is divided into A, B, C, D, and E five phases according to lithology, grain-size, carbonate content, and mineralogical composition. Ages marked in this figure are calibrated ^{14}C ages (cal yr BP).

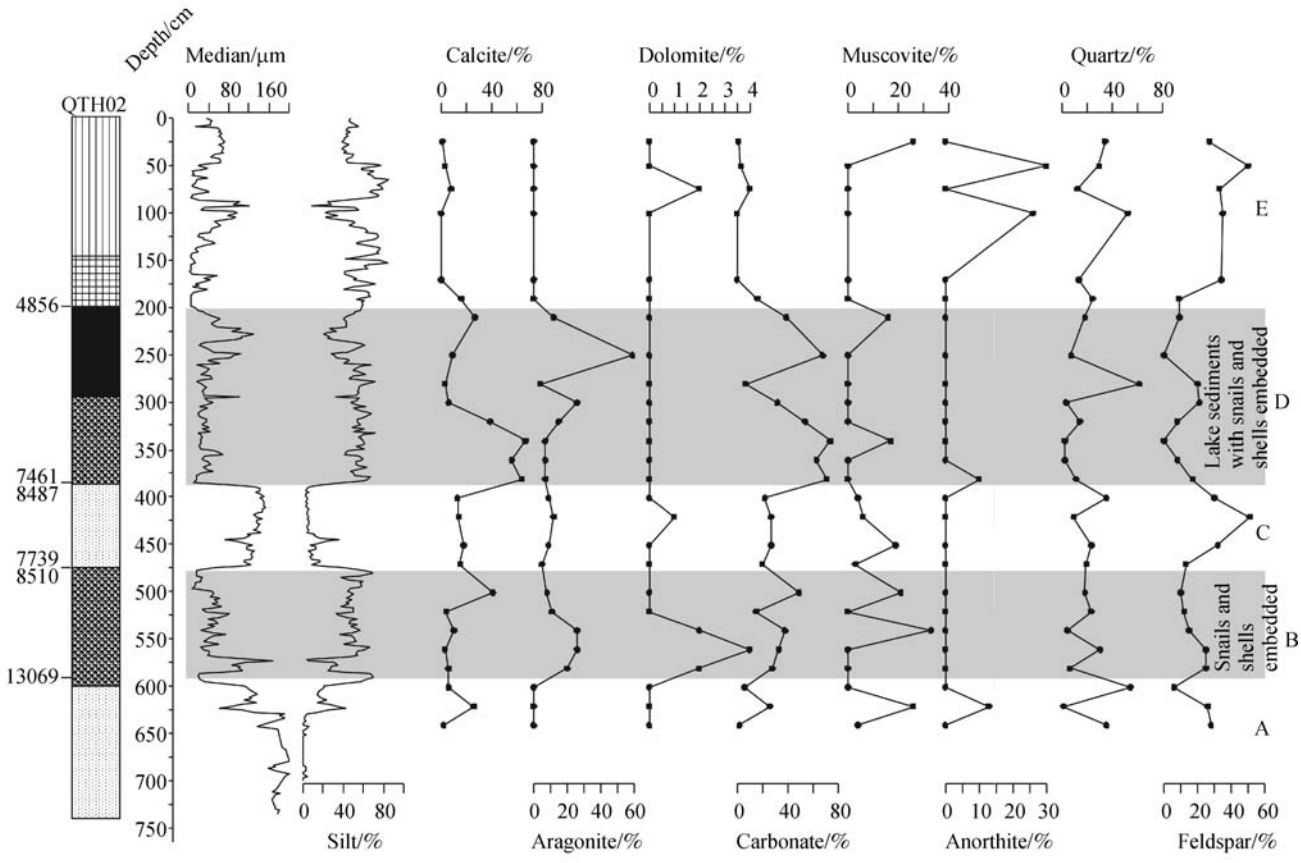

Fig. 4 Percentages of silt content (%), median grain-size (μm), carbonate content (%) and main mineralogical component in the QTH02 section, plotted against the depth. The grey bars indicate typical lacustrine layers with high carbonate content. The section is divided into A, B, C, D, and E five phases according to lithology, grain-size, carbonate content, and mineralogical composition. Ages marked in this figure are calibrated ^{14}C ages (cal yr BP).

the early and middle Holocene. Totally, the ages from the five sections show that the early and middle Holocene is characterized by lake expansion and typical lacustrine sediment formation. It is still difficult to compare the chronologies of the five sections owing to the relatively loose age control.

4.3 Carbonate content and mineralogical composition

As shown in Figs. 3–7 and Table 2, mineralogical composition and carbonate content in the five sections vary according to lithology and grain-size. Calcite and aragonite are two major carbonate minerals in the QTH01, QTH02, and JTL sections, while the carbonate mineral mainly consists of calcite in the XQ and SKJ sections. Dolomite is another carbonate mineral that can be found in the sediments, but it is only found in some samples and the content is low. The content of dolomite does not affect the variability of carbonate minerals in the five sections. Calcite and aragonite are negatively correlated with each other in the QTH01 and QTH02 section, and positively correlated in the JTL section. According to the field observations of these sections, aragonite content is relatively high in the layers with many snails and shells, which are rarely found in the XQ and SKJ sections. Therefore, the aragonite in Zhuye Lake may come mainly from shells and snails. The relationship between aragonite and calcite depends on the abundance of mollusks and the local depositional environment. Quartz, albite, clinochlore, muscovite, and anorthite are major components of detrital minerals in the five sections, which are all light minerals, easily transported by wind, and commonly found in the surrounding deserts. According to the data of mineralogical composition and carbonate content in Table 2, the phases of typical lacustrine sediments (phases B and D in the QTH01, QTH02, JTL, and SKJ sections; phase A and C in the XQ section) are enriched with carbonate. On the contrary, the carbonate content is very low in other phases, illustrating that the high carbonate content agrees well with strong lake hydrodynamic conditions, which are implied by the silt content and median grain-size. Variability of lake carbonate content is basically associated with lake water evaporation and basin-wide carbonate accumulation. The high carbonate content, accompanied by lake expan-

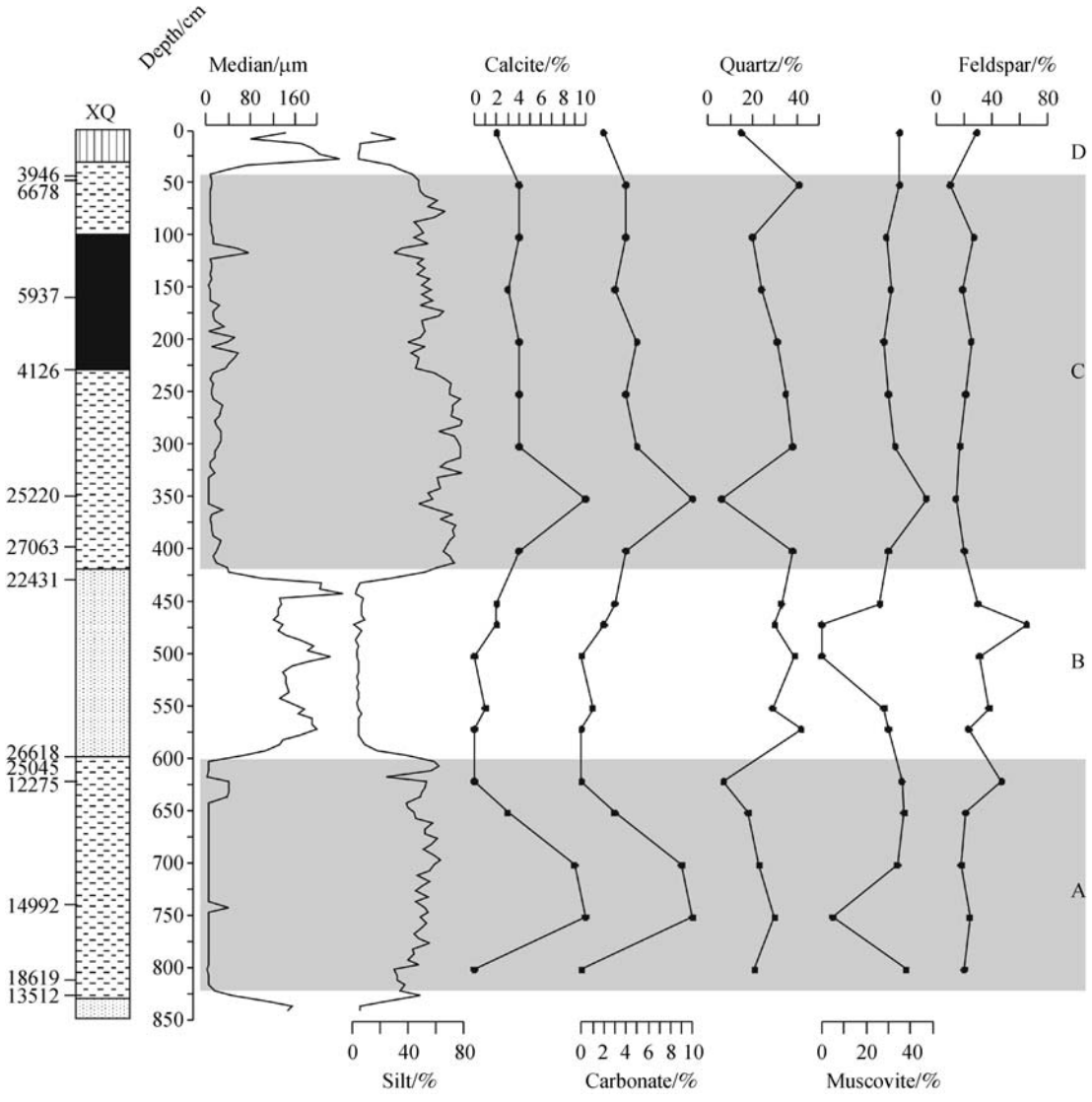

Fig. 5 Percentages of silt content (%), median grain-size (μm), carbonate content (%) and main mineralogical component in the XQ section, plotted against the depth. The grey bars indicate typical lacustrine layers with high carbonate content. The section is divided into A, B, C, and D four phases according to lithology, grain-size, carbonate content, and mineralogical composition. Ages marked in this figure are calibrated ^{14}C ages (cal yr BP).

sion, is likely to be connected with basin-wide carbonate formation and transportation during the period of high effective moisture supply. At most phases of the five sections, the carbonate content is negatively correlated with the contents of quartz and albite, especially in the typical lacustrine sediments. Carbonate enrichment during wet periods may be related to low deposition rates of quartz and feldspars. It is noted that the links between carbonate and detrital minerals are not identical in all the sections. This may be due to local depositional environment and sediment transportation pattern. Carbonate content is relatively low on the top of each section, indicating the low carbonate accumulation rate in aeolian deposits, also indicating a very limited contribution of carbonate minerals.

5 Discussion

Paleo-shorelines and the Late Quaternary lake sediments are widely distributed in the dry lake. Previous studies have shown that the lake level fluctuated frequently during the Late Pleistocene corresponding to climate and environmental changes in the area (Pachur et al., 1995;

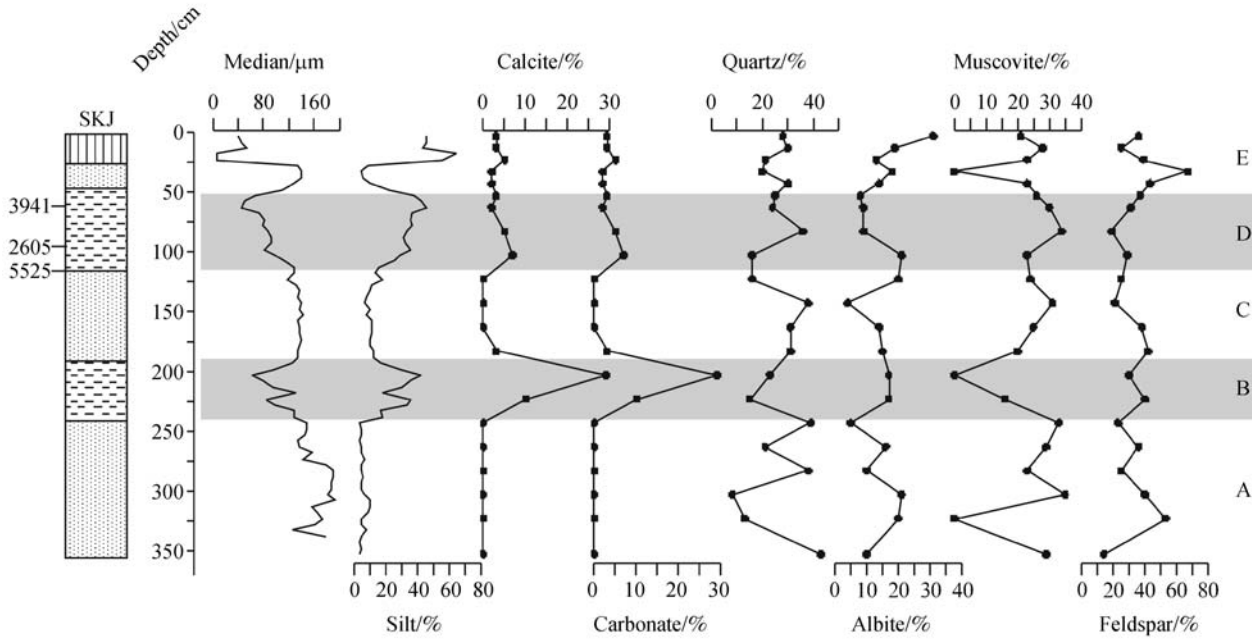

Fig. 6 Percentages of silt content (%), median grain-size (μm), carbonate content (%) and main mineralogical component in the SKJ section, plotted against the depth. The grey bars indicate typical lacustrine layers with high carbonate content. The section is divided into A, B, C, D, and E five phases according to lithology, grain-size, carbonate content, and mineralogical composition. Ages marked in this figure are calibrated ^{14}C ages (cal yr BP).

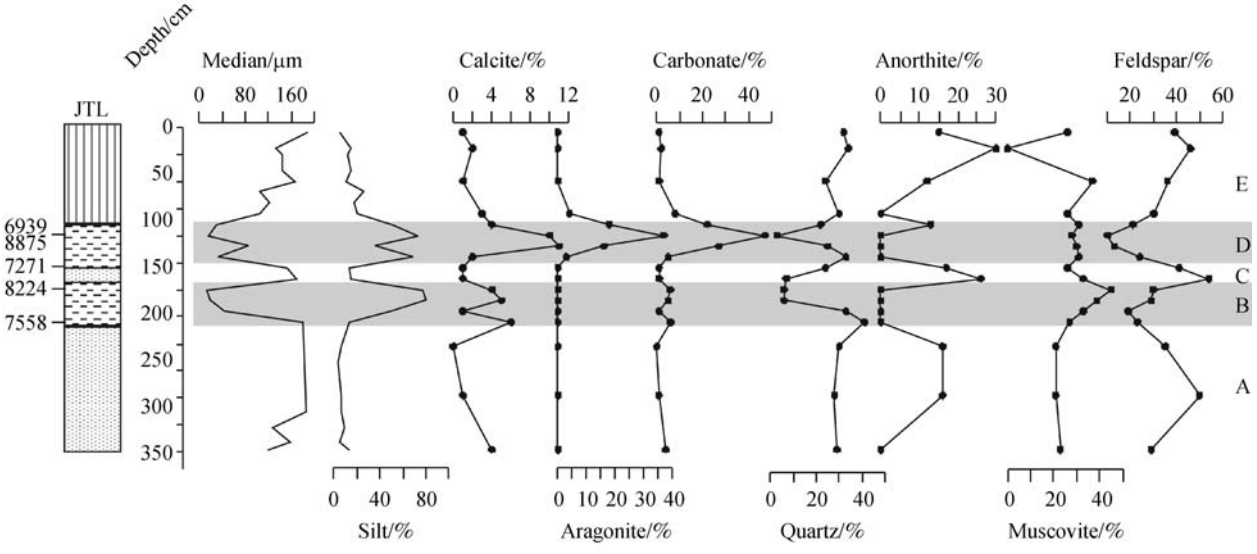

Fig. 7 Percentages of silt content (%), median grain-size (μm), carbonate content (%) and main mineralogical component in the JTL section, plotted against the depth. The grey bars indicate typical lacustrine layers with high carbonate content. The section is divided into A, B, C, D, and E five phases according to lithology, grain-size, carbonate content, and mineralogical composition. Ages marked in this figure are calibrated ^{14}C ages (cal yr BP).

Wünnemann et al., 1998). Zhang et al. (2001, 2002 and 2004) synthesized and updated the radiocarbon dates of the paleo-shorelines and the Late Pleistocene lake sediments in Zhuye Lake and surrounding areas, and then found that the Late Pleistocene lake level reached its highest point during the MIS 3. Their studies focused on the lake geomorphology and chronology for the last 40,000 years. Holocene palynological records in Zhuye Lake showed that the vegetation density was the highest during the mid-Holocene and the runoff increased sharply during the early Holocene (Chen et al., 2006; Zhao et al., 2008; Li et al., 2009). In addition, Chen et al. (2001, 2003) examined the Holocene climate cycles according to lake sediments in the west of the lake basin. Although previous studies have shown a large amount of information on the Late Quaternary lake evolution and climate change, it is still unclear regarding the relationship between long-term lake evolution and carbon cycle. This study presents the lake sediments grain-size data and carbonate content in different locations of the lake basin. The results show that the Holocene lake expansion, which mainly occurred during the early and mid Holocene, was always accompanied by high carbonate content in Zhuye Lake.

Modern rainfall in the drainage basin contains HCO_3^-, Ca^{2+} and Mg^{2+} as major ions, but water from different parts of the drainage area features various chemical composition. Chemical composition of the basin-wide ground and surface water is closely related to the ratio of precipitation and evaporation. From the mountain area to the terminal lake, the water salinity increases, while the ions change from HCO_3^-, Ca^{2+} and Mg^{2+} to Cl^-, SO_4^{2-}, Na^+, Ca^{2+} and Mg^{2+} (Ding and Zhang, 2005). The modern surface and ground water in the terminal lake area is not abundant with carbonate (Liu, 2000; Zheng et al., 2000). The disappearance of the carbonate in the modern terminal lake area is related to strong evaporation and the arid environment. However, Zhuye Lake was enriched with carbonate during the early and mid Holocene, when the lake water chemical composition was similar to rainfall. As a result, the ratio of precipitation and evaporation in the drainage area is completely different between the early-mid Holocene and modern times. The relatively wet environments are good for inorganic carbon accumulation in arid China based on the millennial-scale relationship between lake evolution and carbonate content. Li et al. (2009) have examined organic carbon content in the Holocene Zhuye Lake sediments. Their results indicated that the high organic carbon content also agrees well with lake expansion and abundant basin-wide precipitation. As a result, Zhuye Lake plays a role of carbon sinks both on inorganic and organic carbon during the wet periods. In northwest China and arid Central Asia, precipitation has increased over the past several decades (Shi et al., 2007; Piao et al., 2010). Some lakes have grown and river runoff has increased, although these changes could have a significant contribution from melting glaciers (Shi et al., 2007; Li et al., 2008). The recent wetter trend in arid China can boost the carbon sink function of these areas according to this study.

Zhuye Lake basin is surrounded by the Tengger Desert and the Badain Jaran Desert (Fig. 1). Li (2011) has studied mineralogical composition of surface samples from the two deserts. In the Badain Jaran Desert, quartz and feldspar are two major mineralogical components, averaging 61.13% (30.73%–80.10%) and 19.75% (11.00%–33.67%), based on their study from 70 samples. While the results from the Tengger Desert are similar to those from the Badain Jaran Desert, the average contents for quartz and feldspar are 61.55% (53.00%–69.00%) and 28.58% (23%–35%) according to 70 samples. In this study, quartz and feldspar (mainly albite and anorthite) are also major components for detrital minerals in the five sections. The average quartz contents are 21.40%, 20.73%, 28.14%, 26.00% and 23.94%, while the average feldspar contents are 24.42%, 20.92%, 28.14%, 33.95% and 31.12% for the QTH01, QTH02, XQ, SKJ and JTL sections (Figs. 3–7 and Table 2). In addition, both quartz and feldspar are light minerals that are easily transported by wind; it is therefore inferred that in addition to fluvial fluxes from the catchment eolian transportation processes may play a further role. Besides, the carbonate content is negatively correlated with the contents of quartz and albite in most typical lacustrine sediments; therefore, the lake expansion and basin-wide carbonate accumulation can prevent the wind transportation of quartz and feldspar.

Located in the marginal region of the Asian summer monsoon, climate change of Zhuye Lake is sensitive to the Holocene Asian monsoon evolution (Zhao, 1983; Wang et al., 2005b). The strong Asian summer monsoon during the early and middle Holocene is widely recorded in southern China and the Qinghai-Tibet Plateau (Morinaga et al., 1993; Dykoski et al., 2005; Shen et al., 2005; Wang et al., 2005b; Morrill et al., 2006; Liu et al., 2007; Cai et al., 2010). This pattern closely follows changes of the Holocene summer insolation in low latitudes (Berger and Loutre, 1991). While the Holocene effective moisture change in arid Central Asia reaches an optimal condition during the mid-Holocene (Fowell et al., 2003; Wünnemann et al., 2006; Chen et al., 2008; Liu et al., 2008b). Taking the location of Zhuye Lake into account, the lake expansion during the early and middle Holocene can be affected by the combined effect of the Asian summer monsoon and the westerly winds from Central Asia. More work regarding high-resolution climate reconstruction and climate dynamics in this area is still needed to separate the influences from the monsoon and the westerlies, which is important for projecting the future climate and carbon cycle in arid China.

6 Conclusions

Carbonate content and mineralogical composition were analyzed from sediment samples in different locations of Zhuye Lake since the Late Glacial for detecting the relationship between lake evolution and inorganic carbon cycle. Lake expansion mainly occurs during the early and middle Holocene according to the lithology, grain-size, and chronologies from the QTH01, QTH02, XQ, SKJ, and JTL sections, while the wet environment causes carbonate enrichment in the terminal lake of the drainage area. The carbonate accumulation during wet periods can be associated with high basin-wide precipitation that leads to the surface carbonate redistribution. Calcite and aragonite are two main components for the lake carbonate, and aragonite likely comes from shells and snails based on the observation of those sediment samples. Furthermore, basin-wide vegetation productivity is generally high during wet periods in arid China. The organic carbon content was also proven to highly correspond to the high carbonate content in Zhuye Lake. Overall, this drainage area plays a role of carbon sinks during the wet periods of Holocene. In addition, a recent warmer and wetter trend in northwest China may favor carbon sinking in those regions.

Acknowledgements We thank the editor and reviewers for their constructive comments and suggestions for improving our paper. This research was supported by the National Natural Science Foundation of China (Grant Nos. 41371009 and 41001116) and the Fundamental Research Fund for the Central Universities (Nos. lzujbky-2013-127 and lzujbky-2013-129).

References

Berger A, Loutre M F (1991). Insolation values for the climate of the last 10 million years. Quat Sci Rev, 10(4): 297–317

Brown T A, Nelson D E, Mathewes R W, Vogel J S, Southon J R (1989). Radiocarbon dating of pollen by accelerator mass spectrometry. Quat Res, 32(2): 205–212

Cai Y, Tan L, Cheng H, An Z, Edwards R L, Kelly M J, Kong X, Wang X (2010). The variation of summer monsoon precipitation in central China since the last deglaciation. Earth Planet Sci Lett, 291(1–4): 21–31

Chen F H, Cheng B, Zhao Y, Zhu Y, Madsen D B (2006). Holocene environmental change inferred from a high-resolution pollen record, Lake Zhuyeze, arid China. Holocene, 16(5): 675–684

Chen F H, Wu W, Holmes J, Madsen D B, Zhu Y, Jin M, Oviatt J G (2003). A mid-Holocene drought interval as evidenced by lake desiccation in the Alashan Plateau, Inner Mongolia, China. Chin Sci Bull, 48(14): 1401–1410

Chen F H, Yu Z C, Yang M L, Ito E, Wang S M, Madsen D B, Huang X Z, Zhao Y, Sato T, Birks H J B, Boomer I, Chen J H, An C B, Wünnemann B (2008). Holocene moisture evolution in arid central Asia and its out-of-phase relationship with Asian monsoon history. Quat Sci Rev, 27: 351–364

Chen F H, Zhu Y, Li J, Shi Q, Jin L, Wünemann B (2001). Abrupt Holocene changes of the Asian monsoon at millennial-and centennial-scales: evidence from lake sediment document in Minqin Basin, NW China. Chin Sci Bull, 46(23): 1942–1947

Chen J A, Wan G J, Zhang D, Zhang F, Huang R (2004). Environmental records of different time scales in lake-sediments: grain-size of sediments. Sci China Ser D, 47: 954–960

Chen L H, Qu Y G (1992). Water-land Resources and Reasonable Development and Utilization in the Hexi Region. Beijing: Science Press (in Chinese)

China Meteorological Administration (1994). Atlas of the Climatic Resources of China. Beijing: China Atlas Press (in Chinese)

Dean W E (1999). The carbon cycle and biogeochemical dynamics in lake sediments. J Paleolimnol, 21(4): 375–393

Ding H, Zhang J (2005). Goechemical properties and evolution of groundwater beneath the Hexi Corridor, Gansu Province. Arid Zone Research, 22: 24–28 (in Chinese)

Dykoski C A, Edwards R L, Cheng H, Yuan D, Cai Y, Zhang M, Lin Y, Qing J, An Z, Revenaugh J (2005). A high-resolution, absolute-dated Holocene and deglacial Asian monsoon record from Dongge Cave, China. Earth Planet Sci Lett, 233(1–2): 71–86

Fowell S J, Hansen B C S, Peck J A, Khosbayar P, Ganbold E (2003). Mid to late-Holocene climate evolution of the Lake Telmen basin, North Central Mongolia, based on palynological data. Quat Res, 59 (3): 353–363

Gasse F, Arnold M, Fontes J C, Fort M, Gibert E, Huc A, Li B, Li Y, Liu Q, Melieres F, van Campo E, Wang F, Zhan Q (1991). A 13,000 year climate record from western Tibet. Nature, 353(6346): 742–745

Gierlowski-Kordesch E, Kelts K (1994). Global Geological Record of Lake Basins. Cambridge: Cambridge University Press

Gorham E, Dean W E, Sanger J E (1983). The chemical composition of lakes in the north-central United States. Limnol Oceanogr, 28(2): 287–301

Hammer U T (1986). Saline Lake Ecosystems of the World. Boston: Junk Publishers

Jiang W Y, Liu T S (2007). Timing and spatial distribution of mid-Holocene drying over northern China: Response to a southeastward retreat of the East Asian Monsoon. J Geophys Res, D, Atmospheres, 112(D24): 1–8

Lenton T M (2000). Land and ocean carbon cycle feedback effects on global warming in a simple Earth system model. Tellus, 52(5): 1159–1188

Lerman A (1978). Lake: Chemistry, Geology, Physics. Berlin: Springer–Verlag

Li E (2011). Comparative study of the sediment characteristics in the Badain Jaran and Tengger Deserts. Xi'an: Doctoral Thesis of Shanxi Normal University (in Chinese)

Li X, Cheng G, Jin H, Kang E, Che T, Jin R, Wu L, Nan Z, Wang J, Shen Y (2008). Cryospheric change in China. Global Planet Change, 62(3–4): 210–218

Li Y, Wang N, Cheng H, Zhao Q, Long H (2009). Holocene environmental change in the marginal area of the Asian monsoon: a record from Zhuye Lake, NW China. Boreas, 38(2): 349–361

Liu C L, Wang M L, Jiao P C, Li S D, Chen Z (2006). Features and formation mechanism of faults and potash-forming effect in the Lop Nur salt lake, Xinjiang, China. Acta Geol Sin, 80: 936–943

Liu X Q, Dong H L, Rech J A, Matsumoto R, Yang B, Wang Y B (2008a). Evolution of Chaka Salt Lake in NW China in response to climatic change during the latest Pleistocene–Holocene. Quat Sci Rev, 27(7–8): 867–879

Liu X Q, Herzschuh U, Shen J, Jiang Q, Xiao X (2008b). Holocene environmental and climatic changes inferred from Wulungu Lake in northern Xinjiang, China. Quat Res, 70(3): 412–425

Liu X Q, Shen J, Wang S M, Wang Y B, Liu W G (2007). Southwest monsoon changes indicated by oxygen isotope of ostracode shells from sediments in Qinghai Lake since the late Glacial. Chin Sci Bull, 52(4): 539–544

Liu Z (2000). Research on material composition of Salt Lakes in Tengger Desert region. Journal of Salt Lake Research, 8: 21–26 (in Chinese)

Matter M, Anselmetti F S, Jordanoska B, Wagner B, Wessels M, Wuest A (2010). Carbonate sedimentation and effects of eutrophication observed at the Kalista subaquatic springs in Lake Ohrid (Macedonia). Biogeosciences, 7(11): 3755–3767

McConnaughey T E D A, Labaugh J W, Rosenberry D O, Striegl R G, Reddy M M, Schuster P F, Carter V (1994). Carbon budget for a groundwater-fed lake: calcification supports summer photosynthesis. Limnol Oceanogr, 39(6): 1319–1332

Meyers P A, Ishiwatari R (1993). Lacustrine organic geochemistry—an overview of indicators of organic matter sources and diagenesis in lake sediments. Org Geochem, 20(7): 867–900

Mischke S, Aichner B, Diekmann B, Herzschuh U, Plessen B, Wünnemann B, Zhang C (2010). Ostracods and stable isotopes of a late glacial and Holocene lake record from the NE Tibetan Plateau. Chem Geol, 276(1–2): 95–103

Moore P D, Webb J A, Collinson M E (1991). Pollen Analysis. Oxford: Blackwell

Morinaga H, Itota C, Isezaki N, Goto H, Yaskawa K, Kusakabe M, Liu J, Gu Z, Yuan B, Cong S (1993). Oxygen-18 and carbon-13 records for the last 14 000 years from lacustrine carbonates of Siling-Co (lake) in the Qinghai-Tibetan Plateau. Geophys Res Lett, 20(24): 2909–2912

Morrill C, Overpeck J T, Cole J E, Liu K, Shen C, Tang L (2006). Holocene variations in the Asian monsoon inferred from the geochemistry of lake sediments in central Tibet. Quat Res, 65(2): 232–243

Pachur H J, Wünnemann B, Zhang H (1995). Lake Evolution in the Tengger Desert, Northwestern China, during the last 40,000 Years. Quat Res, 44(2): 171–180

Peng Y J, Xiao J L, Nakamura T, Liu B L, Inouchi Y (2005). Holocene East Asian monsoonal precipitation pattern revealed by grain-size distribution of core sediments of Daihai Lake in Inner Mongolia of north-central China. Earth Planet Sci Lett, 233(3–4): 467–479

Piao S, Ciais P, Huang Y, Shen Z, Peng S, Li J, Zhou L, Liu H, Ma Y, Ding Y, Friedlingstein P, Liu C, Tan K, Yu Y, Zhang T, Fang J (2010). The impacts of climate change on water resources and agriculture in China. Nature, 467(7311): 43–51

Schmalz R F (1966). Environments of marine evaporite deposition. Miner Ind, 35: 1–7

Schnurrenberger D, Russell J, Kelts K (2003). Classification of lacustrine sediments based on sedimentary components. J Paleolimnol, 29(2): 141–154

Shen J, Liu X, Wang S, Matsumoto R (2005). Palaeoclimatic changes in the Qinghai Lake area during the last 18000 years. Quat Int, 136(1): 131–140

Shi Y, Shen Y, Kang E, Li D, Ding Y, Zhang G, Hu R (2007). Recent and future climate change in northwest China. Clim Change, 80(3–4): 379–393

Sun D (1990). “Tear Drop Pattern” potash deposits in lacustrine facies. Chin J Oceanology Limnol, 8(1): 50–65

Sun D, Bloemendal J, Rea D K, Vandenberghe J, Jiang F, An Z, Su R (2002). Grain size distribution function of polymodal sediments in hydraulic and Aeolian environments and numerical partitioning of the sedimentary components. Sediment Geol, 152(3–4): 263–277

Wang H (1987). The water resources of lakes in China. Chin J Oceanology Limnol, 5(3): 263–280

Wang K, Jiang H, Zhao H (2005a). Atmospheric water vapor transport from westerly and monsoon over the Northwest China. Advances in Water Science, 16: 432–438 (in Chinese)

Wang Y, Cheng H, Edwards R L, He Y, Kong X, An Z, Wu J, Kelly M J, Dykoski C A, Li X (2005b). The Holocene Asian monsoon: links to solar changes and North Atlantic climate. Science, 308(5723): 854–857

Wen R L, Xiao J L, Chang Z G, Zhai D Y, Xu Q H, Li Y C, Itoh S (2010). Holocene precipitation and temperature variations in the East Asian monsoonal margin from pollen data from Hulun Lake in northeastern Inner Mongolia, China. Boreas, 39(2): 262–272

Williams W D (1991). Chinese and Mongolian saline lakes: a limnological overview. Hydrobiologia, 210(1–2): 39–66

Wünnemann B, Mischke S, Chen F H (2006). A Holocene sedimentary record from Bosten Lake, China. Palaeogeogr Palaeoclimatol Palaeoecol, 234(2–4): 223–238

Wünnemann B, Pachur H J, Zhang H C (1998). Climatic and environmental changes in the deserts of Inner Mongolia, China, since the Late Pleistocene. In: Alsharhan A S, Glennie K W, Whittle G L, Kendall C G St C, eds. Quaternary Deserts and Climatic Changes. Balkema, Rotterdaman, 381–394

Xiao J L, Si B, Zhai D Y, Itoh S, Lomtatidze Z (2008). Hydrology of Dali Lake in central-eastern Inner Mongolia and Holocene East Asian monsoon variability. J Paleolimnol, 40(1): 519–528

Xiao J L, Xu Q H, Nakamura T, Yang X L, Liang W D, Inouchi Y (2004). Holocene vegetation variation in the Daihai Lake region of north-central China: a direct indication of the Asian monsoon climatic history. Quat Sci Rev, 23(14–15): 1669–1679

Zhang H C, Ma Y Z, Li J J, Qi Y, Chen G J, Fang H B, Wünnemann B, Pachur H J (2001). Palaeolake evolution and abrupt climate changes during last glacial period in NW China. Geophys Res Lett, 28(16): 3203–3206

Zhang H C, Peng J L, Ma Y, Chen G J, Feng Z D, Li B, Fan H F, Chang F Q, Lei G L, Wünnemann B (2004). Late quaternary palaeolake-levels in Tengger Desert, NW China. Palaeogeogr Palaeoclimatol Palaeoecol, 211(1–2): 45–58

Zhang H C, Wünnemann B, Ma Y Z, Peng J L, Pachur H J, Li L J, Qi Y, Chen G J, Fang H B, Feng Z D (2002). Lake level and climate changes between 42,000 and 18,000 ^{14}C yr BP in the Tengger Desert, northwestern China. Quat Res, 58(1): 62–72

Zhao Q (2005). Environment changes of the Shiyang River drainage since the last deglaciation. Lanzhou: Doctoral Thesis of Lanzhou

University (in Chinese)

Zhao S Q (1983). A new scheme for comprehensive physical regionalization in China. Acta Geogr Sin, 38: 1–10 (in Chinese)

Zhao Y, Yu Z, Chen F H, Li J (2008). Holocene vegetation and climate change from a lake sediment record in the Tengger Sandy Desert, northwest China. J Arid Environ, 72(11): 2054–2064

Zheng M, Tang J, Liu J, Zhang F (1993). Chinese saline lakes. Hydrobiogia, 267(1–3): 23–36

Zheng M, Zhao Y, Liu J (2000). Palaeoclimatic indicators of China's Quaternary saline lake sediments and hydrochemistry. Acta Geol Sin, 74: 259–265

Zhou W, Donahua D J, Jull A J T (1999). Radiocarbon AMS dating of pollen concentrated from eolian sediments: implications for monsoon climate change since the late Quaternary. Radiocarbon, 39: 19–26